

# Ferromagnetic features on zero-bias conductance peaks in ferromagnet/insulator/superconductor junction

Nobukatsu Yoshida\* and Masashi Yamashiro†

*Department of Liberal Arts and Basic Sciences, College of Industrial Technology,  
Nihon University, 2-11-1 Shin-ei, Narashino, Chiba 275-8576, Japan*

(Dated: October 31, 2018)

We present a general formula for tunneling conductance in ballistic ferromagnet/ferromagnetic insulator/superconductor junctions where the superconducting state has opposite spin pairing symmetry. The formula can involve correctly a ferromagnetism has been induced by effective mass difference between up- and down-spin electrons. Then, this effective mass mismatch ferromagnet and standard Stoner ferromagnet have been employed in this paper. As an application of the formulation, we have studied the tunneling effect for junctions including spin-triplet  $p$ -wave superconductor, where we choose a normal insulator for the insulating region whereas our formula can treat a ferromagnetic insulator. Then, we have been able to devote our attention to features of ferromagnetic metal. The conductance spectra show a clear difference between two ferromagnets depending upon the way of normalization of the conductance. Especially, a essential difference is seen in zero-bias conductance peaks reflecting characteristics of each ferromagnets. From obtained results, it will be suggested that the measurements of the tunneling conductance in the junction provide us a useful information about the mechanism of itinerant ferromagnetism in metals.

PACS numbers: 72.25.-b, 74.25.F-, 74.20.Rp

## I. INTRODUCTION

Andreev reflection(AR), which occurs at the interface of the junctions involving superconductors, is one of the most important elemental processes in the transport through the superconducting junctions [1]. A theory of transport taking into account the AR was formulated by Blonder, Tinkham and Klapwijk referred to as BTK theory[2]. The BTK theory enables us to probe the pairing state of superconductors. For example, for a junction consists of a normal metal and an unconventional superconductor, the quantum interference effect between the injected and the Andreev reflected particles, which feel mutually the different sign of superconducting pair potential through the scattering event at the interface of the junction, forms the so-called zero-energy Andreev bound states(ZABS)[3, 4]. Indeed, the ZABS originated from the  $d$ -wave symmetry of superconducting pair potential have been observed as the zero-bias conductance peaks(ZBCPs) in tunneling experiment of high  $T_C$  cuprate superconductors [5–7] according to theoretical prediction of Tanaka and Kashiwaya(TK) formula[4]. The ZBCPs reflecting the ZABS are the essential feature of the electrical conduction in normal metal/insulator/unconventional superconductor junction and provide us the information of the pairing symmetry of superconductor[8–10]. On the other hand, in ferromagnet/insulator/conventional superconductor junction, the measurements for low energy transport via AR offer the opportunity to probe the magnetic property such as

the polarization of ferromagnetic materials[11–13]. The AR in this junction is suppressed by the exchange field in the ferromagnet layer. As a result, the conductance at low energy of the junction is suppressed responding to the polarization of ferromagnet. The behavior of ZBCPs in ferromagnet/insulator/unconventional superconductor junction have been studied to understand the characteristic properties of unconventional superconductors and to utilize the properties as applications of spintronics[14–16]. In these junctions, the ferromagnet has been described within the Stoner model based on a picture of free electrons. However, in some materials, the other descriptions of ferromagnetism are required. The ferromagnetism kinetically driven by a spin-dependent bandwidth asymmetry, or, equivalently, by an effective mass splitting between  $\uparrow$ - and  $\downarrow$ -spin particles [17–22] is an interesting model giving itinerant ferromagnet.

Recently, Annunziata, et al. analyzed the charge and spin transport in ferromagnet/insulator/superconductor(F/I/S) junctions with taking account above mentioned the spin-dependent bandwidth asymmetry ferromagnet (SBAF) making the effective masses have different values in ferromagnet[23–25]. They clarified that from the knowledge of the critical transmission angle the measurement of the effective mass difference among the particles could be possible[23]. In there, it has been also shown that the F/I/S junction is an effective probe to investigate the mechanism of ferromagnetism and the pairing symmetry of unconventional superconductor. Furthermore, it is suggested that the F/I/S junction can be useful as switching device using the spin current in the case of the symmetry of superconductor is conventional  $s$ -wave case[24] and be possible as a spin-filtering device[25]. They have studied on F/I/S junctions with several types

---

\*Electronic address: yoshida.nobukatsu@nihon-u.ac.jp

†Electronic address: yamashiro.masashi@nihon-u.ac.jp

of superconducting symmetries as the conventional  $s$ -wave, unconventional  $d_{x^2-y^2}$ -wave, and the time reversal symmetry broken  $d_{x^2-y^2} + is$  or  $d_{x^2-y^2} + d_{xy}$  states. Moreover, although zero bias anomaly of differential resistance has been shown experimentally in  $\text{Sr}_2\text{RuO}_4$ -Pt point contact experiment[26], more recently, Kashiwaya et. al.[27] has shown the ZBCP which is direct evidence of the ZABS by tunneling spectroscopic experiment of  $\text{Sr}_2\text{RuO}_4$ -Au junction. There is much interest and importance to investigate problems on spin triplet  $p$ -wave symmetry nature because the  $p$ -wave pairing, especially, a chiral  $p_x \pm ip_y$  state breaking time-reversal symmetry is one of the best candidates for bulk superconducting state of  $\text{Sr}_2\text{RuO}_4$  [27–34].

In this paper, a formulation of the tunneling conductance for charge and spin currents in ferromagnet/ferromagnetic-insulator/superconductor (F/FI/S) junctions will be presented by taking the effective mass difference leading the spin-band asymmetry between  $\uparrow$ - and  $\downarrow$ -spin particles in ferromagnet [23–25] into our previous theory[14]. Although the formulation can be used for singlet and  $S_z = 0$  triplet superconductors, we will study a chiral  $p$ -wave state. Our formula has general form being able to include the ferromagnetic insulator, however, a normal insulator surrounded by the ferromagnet and the superconductor is considered for the insulating layer to get pure characteristic features of a ferromagnetism in a ferromagnet. It is found that the normalized conductance spectra shows a clear difference between Stoner and spin-band asymmetry ferromagnets (STF and SBAF for abbreviation). The present results may be helpful in investigations of the mechanism of ferromagnet.

This paper is organized as follows. In Sec.II we explain a theoretical model and derive a formulation following our previous method based on the BTK theory. The results for ferromagnet/insulator/chiral  $p$ -wave superconductor junctions are presented in Sec.III. Finally the results are summarized in Sec.IV.

## II. MODEL AND FORMULATION

For the model of formulation, we consider a two-dimensional ballistic F/FI/S junction with semi-infinite electrodes shown in figure 1. A flat interface is assumed to be located at  $x=0$ , and the ferromagnetic insulator for up(down) spin is described by a potential  $V_{\uparrow(\downarrow)}(x) = (V_0 + (-)V_{ex})\delta(x)$ , where  $\delta(x)$ ,  $V_0$  and  $V_{ex}$  are the  $\delta$  function, a nonmagnetic barrier amplitude and a magnetic barrier amplitude, respectively.

For the ferromagnetism in the F electrode, we adopt two kinds models of mechanisms shown in Fig2. One of these is the standard Stoner model in which the ferromagnetism is induced by the exchange potential leading to the rigid energy shift between  $\uparrow$ -spin and  $\downarrow$ -spin bands. The other is a spin bandwidth asymmetry model proposed by Hirsch[18], in which the bandwidth is tuned

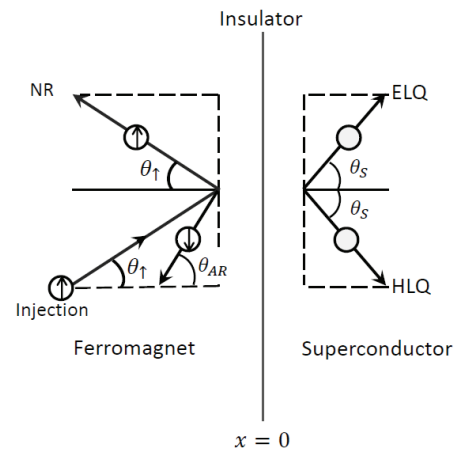


FIG. 1: Schematic illustration of scattering processes of an injected electron with  $\uparrow$ -spin at the F/FI/S ballistic junction. Here,  $\theta_{\uparrow}$ ,  $\theta_{AR}$ , and  $\theta_S$  are injection, Andreev reflection, and transmission angles, respectively. It is assumed that the normal reflection at the interface is totally specular, then normal reflection angle is also given by  $\theta_{\uparrow}$ . For the case of  $\downarrow$ -spin electron, it can be depicted by flipping  $\uparrow$  by  $\downarrow$  in the figure.

relatively by the ratio of the effective masses between  $\uparrow$ - and  $\downarrow$ -spin particles. Although in the following the free particle-like spectra of parabolic type is assumed as normal electronic dispersion relation, we suppose to define the concept of bandwidth for the above description. It implies that there can be some relations between this description and some effective one-band tight binding model permitting the effective masses of carriers being proportional to the inverse of the width of the bands where the carriers get itinerancy. Hence, only giving different values of the masses for  $\uparrow$ - and  $\downarrow$ -spin electrons yields a bandwidth asymmetry.

The spatial dependence of the pair potential is taken as  $\Delta(\mathbf{r}) = \Delta\Theta(x)$  for simplicity. In addition, we consider the  $S_z = 0$  pairing states, where the elements of pairpotential are given by  $\Delta_{\uparrow,\uparrow} = \Delta_{\downarrow,\downarrow} = 0$  and  $\Delta_{\uparrow,\downarrow} = -\Delta_{\downarrow,\uparrow}$  for the singlet pairing state or  $\Delta_{\uparrow,\downarrow} = \Delta_{\downarrow,\uparrow}$  for triplet pairing state. Thus, the effective Hamiltonian(Bogoliubov-de Gennes (BdG) equation) of the system can be reduced the decoupled equation for the eigen states  $(u_{F(S)\uparrow(\downarrow)}(\mathbf{r}), v_{F(S)\downarrow(\uparrow)}(\mathbf{r}))^T$  and is given by

$$\begin{pmatrix} H_0^\sigma(\mathbf{r}) & \Delta(\mathbf{r}) \\ \Delta^*(\mathbf{r}) & -H_0^{\bar{\sigma}}(\mathbf{r}) \end{pmatrix} \begin{pmatrix} u_{F(S)\sigma}(\mathbf{r}) \\ v_{F(S)\bar{\sigma}}(\mathbf{r}) \end{pmatrix} = E \begin{pmatrix} u_{F(S)\sigma}(\mathbf{r}) \\ v_{F(S)\bar{\sigma}}(\mathbf{r}) \end{pmatrix}. \quad (1)$$

Here  $E$  is the energy of the quasiparticle and  $H_0^\sigma(\mathbf{r})$  is the single particle Hamiltonian for  $\sigma$ -spin where  $\bar{\sigma} = -\sigma$ . In the Ferromagnet side, the single particle Hamiltonian is given by  $H_0^\sigma(\mathbf{r}) = -\hbar^2\nabla^2/2m_\sigma - \rho U_{ex} - E_{FM}$  where  $\sigma = \uparrow, \downarrow$ ,  $m_\sigma$  is the effective mass for  $\sigma$ -band particle,  $\rho = +1(-1)$  for  $\uparrow$  ( $\downarrow$ )-spin,  $U_{ex}$  is the exchange potential and  $E_{FM}$  is the Fermi energy. The  $H_0^\sigma$  in

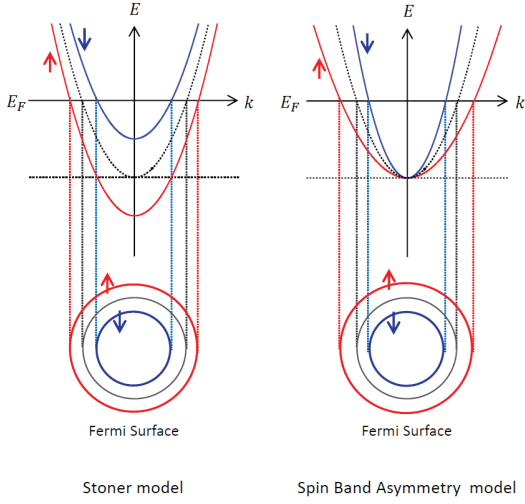


FIG. 2: A sketch of dispersion relation between energy and wave number, and Fermi surface for STF (left side) and for SBAF (right side). It is assumed that free electron model with rigidly energy shift in STF and different effective masses for each spin in SBAF.

the superconductor side is given by  $H_0(\mathbf{r}) = H_0^\sigma(\mathbf{r}) = -\hbar^2 \nabla^2 / 2m_S - E_{FS}$  where the  $m_s$  and  $E_{FS}$  are the effective mass of the quasiparticle and the Fermi energy, respectively. To describe the Fermi surface difference, we assume  $E_{FM} = E_{FS} = E_F$ .

In the following, we apply the quasiclassical approximation where  $E_F \gg (E, \Delta(\mathbf{k}))$  and the  $k$ -dependence of  $\Delta(\mathbf{k})$  is replaced by the angle  $\theta_S$  between the direction of the trajectory of quasiparticles in the superconductor and the interface normal. In the quasiclassical approximation, the wave vectors of  $k_{\uparrow(\downarrow)}$  and  $k_{ELQ(HLQ)}$  are given by  $k_{\uparrow(\downarrow)} = \sqrt{(2m_{\uparrow(\downarrow)}/\hbar^2)(E_F + (-)U_{ex})}$  and  $k_{ELQ(HLQ)} = k_S = \sqrt{2m_S E_F / \hbar^2}$ , respectively, where ELQ (HLQ) indicates electronlike (holelike) quasiparticles. For example, we assume the injection of  $\uparrow$ -spin electrons from the ferromagnet at an angle  $\theta_\uparrow$  to the interface normal as shown in Fig.1. There are four possible scattering trajectories exist; Andreev reflection with angle  $\theta_{AR}$  as holes belonging to  $\downarrow$ -spin band, normal reflection(NR), transmission to superconductor as ELQ, and transmission as HLQ. These four processes are described in same way for  $\downarrow$ -spin electrons with changing the scattering angle  $\theta_\uparrow$  to  $\theta_\downarrow$ . Since the translational symmetry holds along the  $y$ -axis, the parallel momentum components of all trajectories are conserved  $k_\sigma \sin \theta_\sigma = k_{\bar{\sigma}} \sin \theta_{\bar{\sigma}} = k_S \sin \theta_S$ . The angles  $\theta_\sigma$ ,  $\theta_{\bar{\sigma}}$  and  $\theta_S$  differ from each other except when  $U_{ex} = 0$  and  $m_\uparrow = m_\downarrow = m_S$ , which means retroreflectively of AR broken by the exchange field and the effective masses difference. The BdG equations are reduced to the effective one-dimensional equation due to the translational invariance along  $y$ -axis of the Hamiltonian. Thus, the solutions of the BdG equations for  $\sigma$ -spin electron injections are described as

$$\begin{pmatrix} u_{F\sigma}(x < 0) \\ v_{F\bar{\sigma}}(x < 0) \end{pmatrix} = \begin{pmatrix} 1 \\ 0 \end{pmatrix} e^{ik_\sigma x \cos \theta_\sigma} + a_{\bar{\sigma}} \begin{pmatrix} 0 \\ 1 \end{pmatrix} e^{ik_{\bar{\sigma}} x \cos \theta_{\bar{\sigma}}} + b_\sigma \begin{pmatrix} 1 \\ 0 \end{pmatrix} e^{-ik_\sigma x \cos \theta_\sigma} \quad (2)$$

$$\begin{pmatrix} u_{S\sigma}(x > 0) \\ v_{S\bar{\sigma}}(x > 0) \end{pmatrix} = c_\sigma \begin{pmatrix} u_+ \\ v_+ e^{-i\phi_+} \end{pmatrix} e^{ik_S x \cos \theta_S} + d_\sigma \begin{pmatrix} v_- e^{i\phi_-} \\ u_- \end{pmatrix} e^{-ik_S x \cos \theta_S} \quad (3)$$

with

$$u_\pm = \sqrt{\frac{1}{2} \left( 1 + \frac{\Omega_\pm}{E} \right)}, \quad v_\pm = \sqrt{\frac{1}{2} \left( 1 - \frac{\Omega_\pm}{E} \right)}, \quad \Omega_\pm = \sqrt{E^2 - |\Delta_\pm|^2}, \quad (4)$$

$$e^{i\phi_\pm} = \frac{\Delta_\pm}{|\Delta_\pm|}, \quad \Delta_+ = \Delta(\theta_S), \quad \Delta_- = \Delta(\pi - \theta_S) \quad (5)$$

where the probability coefficients  $a_{\bar{\sigma}}$ ,  $b_\sigma$ ,  $c_\sigma$ , and  $d_\sigma$  are for AR, NR, transmission ELQ and HLQ. These coefficients are calculated from the boundary conditions at  $x = 0$ ,

$$u(v)_{F\sigma(\bar{\sigma})}(x = 0) = u(v)_{S\sigma(\bar{\sigma})}(x = 0), \quad (6)$$

$$\frac{\hbar^2}{2m_S} \frac{du_{S\sigma}}{dx} \Big|_{x=0} - \frac{\hbar^2}{2m_\sigma} \frac{du_{F\sigma}}{dx} \Big|_{x=0} = V_\sigma u_{S\sigma}(x = 0) \quad (7)$$

$$\frac{\hbar^2}{2m_S} \frac{dv_{S\bar{\sigma}}}{dx} \Big|_{x=0} - \frac{\hbar^2}{2m_{\bar{\sigma}}} \frac{dv_{F\bar{\sigma}}}{dx} \Big|_{x=0} = V_{\bar{\sigma}} v_{S\bar{\sigma}}(x = 0) \quad (8)$$

As explained in our previous paper, the reflection process depends upon the size relation of the Fermi surfaces between FM and SC. In the following, we will consider a situation where  $k_\downarrow < k_S < k_\uparrow$ , and  $m_\uparrow/m_S = m_S/m_\downarrow$  with  $m_\uparrow > m_S > m_\downarrow$ . Following the BTK theory with taking care of the probability conservation of quasiparticle flow,

$$|b_\sigma|^2 + \frac{v_{f,\bar{\sigma}}}{v_{f,\sigma}} |a_{\bar{\sigma}}|^2 + \frac{v_{s,+}}{v_{f,\sigma}} |c_\sigma|^2 + \frac{v_{s,-}}{v_{f,\sigma}} |d_\sigma|^2 = 1 \quad (9)$$

the conductance  $G_{S,\sigma}^{C(S)}$  for the  $\sigma$ -spin charge(spine) current through the system can be calculated by

$$G_{S,\sigma}^{C(S)} = 1 + (-) \frac{v_{f,\bar{\sigma}}}{v_{f,\sigma}} |a_{\bar{\sigma}}|^2 - |b_\sigma|^2 \quad (10)$$

where  $v_{f,\sigma} = \hbar k_\sigma/m_\sigma$  is the group velocities of the  $\sigma$ -spin

particles in ferromagnet and  $v_{s,+(-)} = \hbar k_S/m_S$  is that of the ELQ (HLQ) in superconductor. It is much worth to note that our conductance formula  $G_{S,\sigma}^{C(S)}$  is different from former works[23–25]. On our way of formulating the conductance as an extension of previous formulation [8, 14] to the present situation, it has to be needed for correct treatment of mass mismatch in a same metal that the coefficient of AR ( $a_{\bar{\sigma}}$ ) should be given by the ratio of group velocities rather than that of wavenumbers as a consequence of conservation law of particle flow. Using the obtained AR ( $a_{\bar{\sigma}}$ ) and NR ( $b_\sigma$ ) coefficients in the same way as the previous paper[14] based on the TK formula[4], the charge(spine) conductance for each spin  $\uparrow$  and  $\downarrow$  can be formulated by

$$G_{S,\uparrow}^{C(S)} = G_{N,\uparrow} \frac{1 - |\Gamma_+\Gamma_-|^2 (1 - G_{N,\downarrow}) + (-)G_{N,\downarrow} |\Gamma_+|^2}{|1 - \Gamma_+\Gamma_- \sqrt{1 - G_{N,\downarrow}} \sqrt{1 - G_{N,\uparrow}} \exp[i(\varphi_\downarrow - \varphi_\uparrow)]|^2} \Theta(|\theta_S| - \theta_C) \\ + [1 - \Theta(|\theta_S| - \theta_C)] G_{N,\uparrow} \frac{1 - |\Gamma_+\Gamma_-|^2}{|1 - \Gamma_+\Gamma_- \sqrt{1 - G_{N,\uparrow}} \exp[i(\varphi_\downarrow - \varphi_\uparrow)]|^2} \quad (11)$$

$$G_{S,\downarrow}^{C(S)} = G_{N,\downarrow} \frac{1 - |\Gamma_+\Gamma_-|^2 (1 - G_{N,\uparrow}) + G_{N,\uparrow} |\Gamma_+|^2}{|1 - \Gamma_+\Gamma_- \sqrt{1 - G_{N,\downarrow}} \sqrt{1 - G_{N,\uparrow}} \exp[i(\varphi_\uparrow - \varphi_\downarrow)]|^2} \Theta(|\theta_S| - \theta_C) \quad (12)$$

with

$$G_{N,\uparrow(\downarrow)} = \frac{4\lambda_{\uparrow(\downarrow)}}{(1 + \lambda_{\uparrow(\downarrow)})^2 + Z_{\uparrow(\downarrow)}^2}, \quad \exp(i\varphi_{\uparrow(\downarrow)}) = \frac{1 - \lambda_{\uparrow(\downarrow)} + iZ_{\uparrow(\downarrow)}}{1 + \lambda_{\uparrow(\downarrow)} + iZ_{\uparrow(\downarrow)}}, \\ Z_{\uparrow(\downarrow)} = \frac{Z_{0,\uparrow(\downarrow)}}{\cos\theta_S}, \quad Z_{0,\uparrow(\downarrow)} = \frac{2m_s(V_0 - (+)V_{ex})}{\hbar^2 k_S}, \quad \Gamma_\pm = \frac{v_\pm}{u_\pm}, \\ \lambda_{\uparrow(\downarrow)} = \sqrt{\gamma^{-1(1)} + \frac{\gamma^{-1/2(1/2)}}{\cos^2\theta_S} (1 - \gamma^{-1/2(1/2)} + (-)\chi)}, \quad (13)$$

where  $\theta_C \equiv \cos^{-1} \sqrt{\gamma^{-1/2}(\chi - 1 + \gamma^{1/2})}$  ( or  $\sin^{-1} \sqrt{\gamma^{-1/2}(1 - \chi)}$  ) is the critical angle of the AR measured in the superconductor side. Here,  $\chi = U_{ex}/E_F$  ( $0 \leq \chi \leq 1$ ) and  $\gamma = m_\uparrow/m_\downarrow \geq 1$ . In the above,  $G_{N,\sigma}$  corresponds to the conductance when the superconductor is in the normal state. We calculate the normalized conductance defined by

$$G_T^{C(S)}(eV) = \frac{\int_{\pi/2}^{\pi/2} d\theta_S \cos\theta_S (P_\uparrow G_{S,\uparrow}^{C(S)} + P_\downarrow G_{S,\downarrow}^{C(S)})}{\int_{\pi/2}^{\pi/2} d\theta_S \cos\theta_S (P_\uparrow G_{N,\uparrow} + P_\downarrow G_{N,\downarrow})} \quad (14)$$

where the polarization  $P_\sigma$  for  $\sigma$ -spin is expressed as

$$P_\uparrow = \frac{\gamma(1 + \chi)}{\gamma(1 + \chi) + 1 - \chi}, \quad P_\downarrow = \frac{1 - \chi}{\gamma(1 + \chi) + 1 - \chi}.$$

It is noted in general that the normalized conductance will be defined alternatively corresponding to the actual experiments.

Above formulas (2.11), (2.12), and (2.14) can reproduce former formulas of tunneling conductance for junctions including triplet superconductor (TS). For  $m_\uparrow = m_\downarrow$ , these equations coincide to that of STF/I/Ts

TABLE I: Numerical values of the magnetization  $M$ , the normalized exchange interaction  $\chi = U_{ex}/E_F$ , and the mass ratio  $\gamma = m_\uparrow/m_\downarrow$ . For the value  $M = 0.25$ , there are two cases, one is pure STF,  $\chi = 0.25$  and  $\gamma = 1$ , and the other is pure SBAF,  $\chi = 0$  and  $\gamma = 5/3$ . All other values of  $M$  are in the same way except the case of  $M = 0$ .

magnetization $M$	exchange Int. $\chi$	mass mismatch $\gamma$
0	0	1
0.25	0.25	1
0.25	0	5/3
0.5	0.5	1
0.5	0	3
0.75	0.75	1
0.75	0	7
0.99	0.99	1
0.99	0	200

junction[14], and for  $m_\uparrow = m_\downarrow$  and  $U_{ex} = 0$ , the conductance formula for N/I/TS junction[8] is reproduced.

### III. RESULTS

At first, we notice about the growth of the magnetization  $M$  for STF or SBAF. Using the polarization  $P_\sigma$ ,  $M$  is given by  $M = P_\uparrow - P_\downarrow$ . For pure STF case ( $\gamma = 1$ ), the magnetization is equal to the magnitude of exchange splitting  $M = \chi (= U_{ex}/E_F)$ . For pure SBAF case ( $\chi = 0$ ), the  $M$  is given by  $M = (\gamma - 1)/(\gamma + 1)$ . Thus, the half metal state in SBAF case is unphysical situation because  $\gamma = \infty$ . Figure 3 shows the  $M$  in SBAF case as a function of  $\gamma$ . It can be seen that the growth rate of  $M$  becomes very gradual over  $\gamma \approx 50$ . From this, one can expect the clear differences of transport properties depending on  $M$  between STF and SBA near the half metallic limit. Hereafter, we call ‘‘strong ferromagnetic regime’’ as a region under and near the half metallic limit.

In the following sub sections, we apply our conductance formula to ferromagnet/insulator/triplet superconductor (F/I/TS) junction (F referred to as STF or SBAF) where  $V_{ex} = 0$ . As the pairing potential, a triplet  $p$ -wave state is employed by choosing  $\Delta_{\uparrow\downarrow}(\theta_S) = \Delta_{\downarrow\uparrow}(\theta_S) = \Delta_0 \exp(i\theta_S)$ ,  $\Delta_{\uparrow\uparrow}(\theta_S) = \Delta_{\downarrow\downarrow}(\theta_S) = 0$  for opposite spin pairing. And in addition, we choose some sets of parameters  $(\chi, \gamma)$  giving the same  $M = \{0, 0.25, 0.5, 0.75, 0.99\}$  shown in Table I so as to get clear characteristics of each ferromagnets.

#### A. Distinction between STF and SBAF

To investigate a consequence of the different mechanism of the magnetization, avoiding any effects of the normal barrier we consider the highly transparent junction in the metallic limit ( $Z_0 = 0$ ). In this case, the normalized total conductances  $G_T^C(eV)$  show same trend that conductance values inside the energy gap  $eV < \Delta_0$  are reduced when the value of magnetization  $M$  is in-

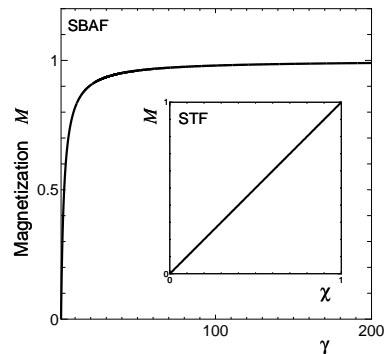


FIG. 3: The magnetization  $M$  as a function of  $\gamma$  in the pure SBAF, and inserted panel is  $M$  as a function of  $\chi$  in the pure STF.

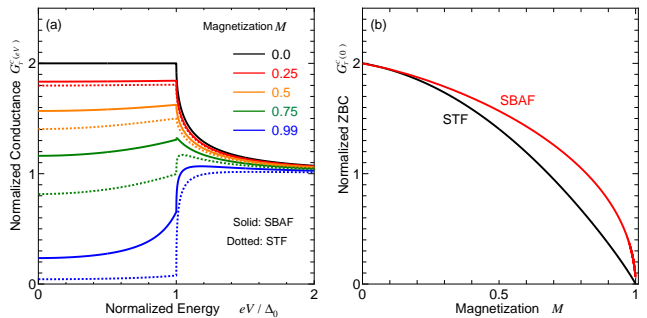


FIG. 4: Normalized conductance spectra for the charge current  $G_T^C(eV)$  in the metallic limit,  $Z = 0$  in (a), and in (b), height of conductance at zero energy is plotted as a function of the magnetization  $M$  for STF (red line) and for SBAF (black line).

creased for both STF and SBAF (Fig.4(a)). It indicates that the retro-reflectivity of the AR is broken due to the induced  $M$ . However, the  $M$  dependence of reduction for  $G_T^C(eV < \Delta_0)$  is different for each of them. The difference can be seen more clearly in the  $M$ -dependence of conductance values at  $eV = 0$ ,  $G_T^C(0)$ , in Fig.4.(b). It is found that the suppression of  $G_T^C(0)$  for SBAF case is weaker rather than that for STF case without weak magnetization regime,  $0.0 \leq M \leq 0.2$  and at half metallic limit,  $M = 1.0$ . To clear the reason of different  $M$  dependence of conductances for SBAF case and STF case, we show the critical angle of AR as a function of  $M$  in Fig.5. The  $\theta_C$  for both SBAF and STF cases decreases with increasing  $M$ . It is found that the difference between angles is getting larger from  $M \sim 0.2$  to  $\sim 0.9$ , and converges to zero at  $M = 1.0$ . For nearly half metallic limit  $M = 0.99$ , the  $\theta_C$  is almost suppressed in the STF case, while there still remains in the SBAF case. The critical angles for STF and SBAF are  $\theta_C = \cos^{-1} \sqrt{M} (= \sin^{-1} \sqrt{1-M})$  and  $\theta_C = \cos^{-1} \sqrt{1 - (\frac{1-M}{1+M})^{1/2}} (= \sin^{-1} \sqrt{(\frac{1-M}{1+M})^{1/2}})$ , respectively. Then, it is clear that  $\theta_C$  in SBAF case is

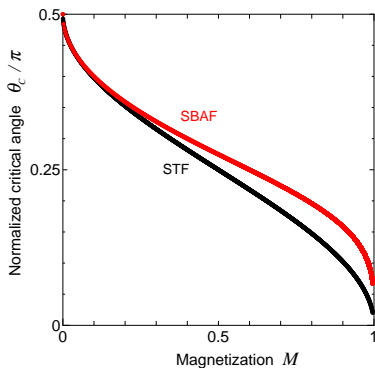


FIG. 5: Critical angles of AR as functions of  $M$  for STF (black line) and for SBAF (red line). As described in main text, these angles are determined by the conservation condition for momenta parallel to the interface,  $k_{\downarrow} \sin \theta_{\downarrow} = k_S \sin \theta_S$ . Such as in the present model, i.e., the ferromagnetism is given by a mismatch in kinetic energy the AR critical angle is determined by  $\theta_C = \theta_S$  for the case of  $\theta_{\downarrow} = \pi/2$  because of satisfying the condition  $k_{\downarrow} < k_S$ .

larger than that in STF case for same  $M$  except non-magnetic state,  $M = 0$  and half metal state,  $M = 1$ . Consequently, as shown in Fig.4, the  $G_T^C(eV < \Delta)$  in SBAF case is larger than that in STF case.

### B. Ferromagnetic feature on ZBCP

It has been shown theoretically that the ZBCP in F/I/S junction would be useful for measuring the magnetization of ferromagnet[14, 15]. In here, we study the validity of the ZBCP for the distinction of ferromagnets. Figure 6 shows the conductance  $G_T^C(eV)$  for the junction in the tunneling limit  $Z = 5$ . The ZBCPs seen in both STF and SBAF cases are attributed to the anisotropy of the pair potential of  $p$ -wave superconductor. For STF case, the previous results[14] have been reproduced(Fig.6(a)). In contrast, there are some differences for SBAF case. Especially, it is found that the conductance near  $eV = 0$  increases slightly with increasing  $M$  (Fig.6(b)). This opposite behavior can be seen more clearly in the  $M$  dependence of ZBCPiFig.6(c). With increasing  $M$ , in contrast to the monotonically decreasing behavior of STF case, the ZBCP in SBAF case increases up to a certain value of  $M$  in strong ferromagnetic regime and then, suddenly decreases toward the half metallic limit where the ZBCPs in both cases are suppressed perfectly. Cause of this opposite behavior could be reduced to the definition of normalization way since the magnitude of ZBCP being a constant value in non-normalized case depends on the conductance as the superconductor is in normal state. There is other definition of normalization by using the AR critical angle measured in the ferromagnet side[14, 15]. However, in that case, the AR critical angle itself depends on and is controlled by the

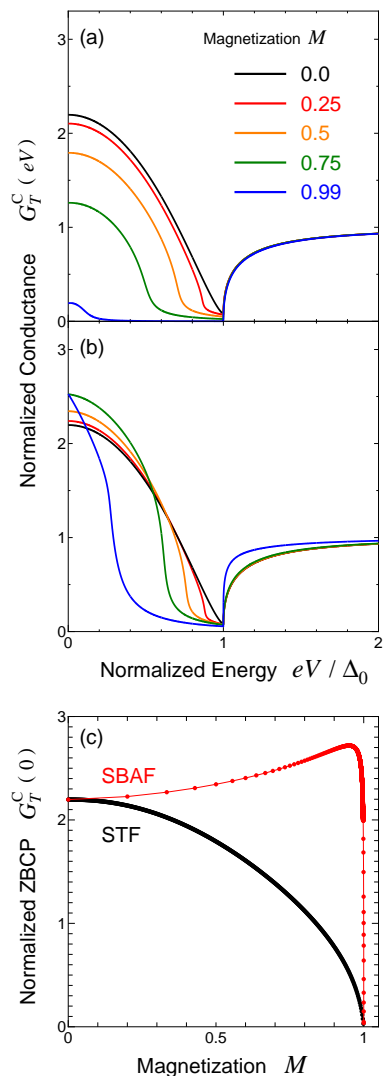


FIG. 6: Normalized conductance spectra of the charge current  $G_T^C(eV)$  in the tunneling limit,  $Z = 5$  for STF/I/TS junction (a) and for SBAF/I/TS junction (b). And in (c), height of ZBCPs is plotted as a function of the magnetization  $M$  for STF (red line) and for SBAF (black line).

magnitude of  $M$ , as a results, even the normalization depends on  $M$ . Accordingly, in order to avoid the influence of  $M$ , we alternatively calculate an angle averaged conductance defined as in the following,

$$Q_S = Q_{S,\uparrow} + Q_{S,\downarrow}$$

$$Q_{S,\sigma} = \frac{\int_{\pi/2}^{\pi/2} d\theta_S \cos \theta_S P_{\sigma} G_{S,\sigma}^C}{\int_{\pi/2}^{\pi/2} d\theta_S \cos \theta_S}.$$

We show the calculated results of the angle averaged conductance  $Q_S$  in Fig.7 which, in both STF and SBAF cases, show same tendency to decrease as increasing  $M$ (Fig.7(a)). Similarly, the ZBCP is decreasing function of  $M$ (Fig.7(b)). It is also shown that the reduction ratio

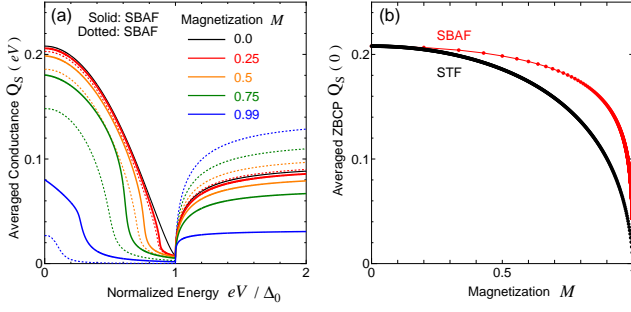


FIG. 7: Angle averaged conductance spectra  $Q_S$  as a function of magnetization (a) and ZBCPs vs. magnetization strength (b) in the tunneling limit  $Z = 5$ . Here, the conductance for SBAF case is indicated as solid line and for STF case is as dotted line.

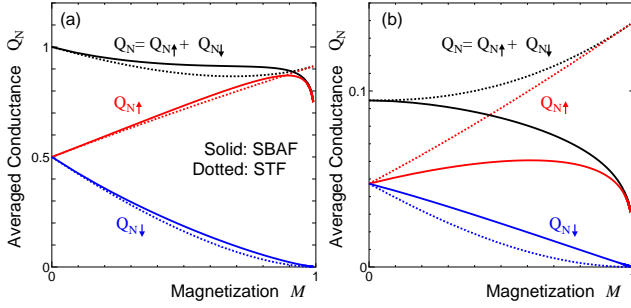


FIG. 8: Magnetization dependence of angle averaged normal conductance  $Q_N$ ,  $Q_{N,\uparrow}$ , and  $Q_{N,\downarrow}$  for SBAF case (solid line) and STF case (dotted line) in the tunneling limit for the case of the superconductor is in normal state, (a) for  $Z = 0$ , (b) for  $Z = 5$ .

differs in each of both cases as same as that in metallic limit. Thus, the opposite behavior seen in normalized conductance would reduce to the conductance in normal state. Therefore, it is noticed that the conductance of the junction for the superconductor being in normal state play an important role on our attention for two different ferromagnetisms.

In order to clarify the difference between STF case and SBAF case more, we calculate the conductance in ferromagnet/normal metal (F/I/N) junction for both in metallic and in tunneling limits. The angle averaged conductance in F/I/N junction  $Q_N = \sum_{\sigma} Q_{N,\sigma}$  is defined in similar way to that in F/I/S junction replacing  $G_{S,\sigma}^C$  by  $G_{N,\sigma}^C$ . The calculated results of  $Q_{N,\sigma}$  for both  $Z_0 = 0$  and  $Z_0 = 5$  are shown in Fig.8. The angle resolved conductance  $G_{N,\sigma}^C$  for  $\sigma$ -spin is rewritten by  $G_{N,\sigma}^C = 4 \cos \theta_S \tilde{\lambda}_{\sigma} / ((\cos \theta_S + \tilde{\lambda}_{\sigma})^2 + Z_{0,\sigma}^2)$  where  $\tilde{\lambda}_{\sigma} = \sqrt{\cos^2 \theta_S + \rho \chi}$  in STF/I/N and  $\tilde{\lambda}_{\sigma} = \gamma^{-\rho/2} \sqrt{\cos^2 \theta_S + (\gamma^{\rho/2} - 1)}$  in SBAF/I/N junctions. Here, we mention properties of  $M$ -dependence of  $G_{N,\sigma}^C$  through  $\chi$  or  $\gamma$  in advance of descriptions about

$Q_N$ . In STF/I/N junction, the  $G_{N,\uparrow}^C$  increases following growth of the magnetization, i.e., with increasing  $\chi$  since the gain of Fermi energy due to the band shift is larger than the Fermi surface effect[14] acting as an effective barrier between STF and normal metal, under the conservation of the momentum along  $y$ -direction. On the other hand, because there is no Fermi energy gain from spread of the band width due to the effective mass mismatch in SBAF and the influence of the effective barrier arising from the Fermi surface effect becomes stronger with the increase of  $\gamma$ , the  $G_{N,\uparrow}^C$  in SBAF/I/N junction decreases with increasing  $\gamma$  and become zero in the limit of  $\gamma \rightarrow \infty$ .  $G_{N,\downarrow}^C$  for both STF and SBAF cases decreases with increasing the magnetization caused by  $\chi$  or  $\gamma$ .

In the metallic limit  $Z_0 = 0$  (Fig.8(a)), it is found that the  $Q_{N,\uparrow}$  in STF/I/N junction increases with increasing  $M$  in contrast to  $Q_{N,\downarrow}$  decreasing toward zero in half metal state. In this case,  $M$  is given directly as  $M = \chi$ . Thus, the total conductance  $Q_N = Q_{N,\uparrow} + Q_{N,\downarrow}$  is reduced slightly by the Fermi surface effect with increasing  $M$  up to  $\sim 0.7$ . In SBAF/I/N junction, we can see similar behavior in  $Q_{N,\uparrow(\downarrow)}$ . The increase of  $Q_{N,\uparrow}$  is owing to  $P_{\uparrow}$  which is an increasing function of  $\gamma$ . However, near the half metallic limit,  $Q_{N,\uparrow}$  reduces rapidly reflecting the behavior of  $G_{N,\uparrow}^C$  which is a decreasing function of  $M$  toward zero at  $M = 1$  ( $\gamma = \infty$ ) as mentioned above. Thus, as shown in Fig.4, the  $G_T^S(eV)$  in SBAF/I/S junction decreases slowly with increasing  $M$  with comparing to that in STF/I/S junction. The difference between STF and SBAF becomes more clearly in the tunneling limit  $Z = 5$ (Fig.8(b)). With increasing  $M$ ,  $Q_{N,\sigma}$  in STF case varies in rapidly rather than that in SBAF case. This is a difference of a barrier effect felt by particles with  $\sigma$ -spin in each cases. The barrier potential simply becomes relatively lower for particles with  $\uparrow$ -spin and higher for particles with  $\downarrow$ -spin in the STF case due to the rigid Fermi energy shift. However, the particles in SBAF directly feel the barrier potential because there is no shift of the Fermi energy. Thus, in SBAF/I/N junction, the increase of the magnitude of  $Q_{N,\uparrow}$  due to  $P_{\uparrow}$  is suppressed by the Fermi surface effect and barrier potential and then,  $Q_{N,\uparrow}$  is getting lower with increasing  $M$  in contrast to the STF case. Therefore, the  $Q_N$  in SBAF/I/N junction shows the opposite behavior of that in STF/I/N junction. As a result, the normalized conductance  $G_T^S(eV)$  in SBAF/I/S junction increases due to the reduction of the  $Q_N$  depending on  $M$  (Fig.6(b)-(c)). Indeed, as shown in Fig.7, the angle averaged conductance  $Q_S(eV)$ s for both STF and SBAF case show same trend on varying  $M$ . Thus, it can be conclude that the measurement of  $Q_N$  will be also useful to identify the STF and SBAF. However, we emphasize that the measurement of ZBCP originated from ZABS is more powerful probe to investigate ferromagnet than that of  $Q_N$ . Because, two  $Q_N$ s seemingly show drastically different behavior depending on  $M$  for enough large  $Z_0$  (Fig.8(b)), by carefully looking of the figure, differences of each values of  $Q_N$ s are not so large for same  $M$  except strong ferromagnetic regime. Therefore, it seems

that an experimental distinction will become more difficult on measurement of  $Q_N$ . The ZBCP is getting more clear for larger  $Z_0$ , then which can be expected to play a role of good manifestation of the difference of STF and SBAF.

#### IV. SUMMARY

In summary, we have derived a formula of the tunneling conductance in ferromagnet/ferromagnetic-insulator/superconductor with antiparallel spin pairing junction by extending our previous theory for standard Stoner ferromagnet (STF) so as to include spin-band asymmetry ferromagnet (SBAF) originated from effective mass mismatch between particles with opposite spins. Applying the formulation to ferromagnet/insulator/ $p$ -wave superconductor junctions, differences between pure STF and pure SBAF have been investigated intensively. We found that, with growing the magnetization, the difference becomes clear in tunneling conductance. The clarity of difference between STF and SBAF depends on the way of normalization of conductance and comes out more clearly in ZBCP near

half-metallic limit. The obtained results suggest that the measurement of ZBCP may be useful for discriminating mechanism of ferromagnetism.

Although our formulation includes the ferromagnetic insulator, we have studied only the normal insulating barrier case in this paper. The spin-filtering effect have been expected in the ferromagnetic insulator[14] or in ferromagnet given by the effective mass mismatch[25]. Then, as an interesting future problem we will study extensively the spin-filtering effect in junctions of including both ferromagnetic insulator and mass mismatch ferromagnet connected to superconductors of  $s$ -,  $d$ -wave and broken time reversal symmetry pairing states. Moreover, it will be an important issue that the proximity effect is taken into account to the present formulation by carrying out the self-consistent calculation of the pairing potential in order to analyze the actual experiments. Indeed, the ZBCP have been observed in tunneling experiment of F/I/ $d$ -wave superconductor junction[35]. And also, ZBCP in  $\text{Sr}_2\text{RuO}_4$  junction has been observed[27], then, tunneling spectroscopy of F/I/ $\text{Sr}_2\text{RuO}_4$  junction seems to be realized in near future. Our conductance formula can apply to such situations easily and get comparable results to experimental one.

- 
- [1] A. F. Andreev, Zh. Eksp. Teor. Fiz. **46**, 1823 (1964). [Sov. Phys. JETP **19**, 1228 (1964)].
- [2] G. F. Blonder, M. Tinkham, and T. m. Klapwijk, Phys. Rev. B **25**, 4515 (1982).
- [3] C. R. Hu, Phys. Rev. Lett. **72**, 1526 (1994).
- [4] Y. Tanaka and S. Kashiwaya, Phys. Rev. Lett. **74**, 3451 (1995).
- [5] S. Kashiwaya, Y. Tanaka, M. Koyanagi, H. Takashima, and K. Kajimura, Phys. Rev. B **51**, 1350 (1995).
- [6] S. Kashiwaya and Y. Tanaka, Rep. Prog. Phys. **63**, 1596 (2000), Phys. Rev. B **56**, 7847 (1997).
- [7] G. Deutscher, Rev. Mod. Phys. **B 238**, 109 (2005).
- [8] M. Yamashiro, Y. Tanaka, and S. Kashiwaya, Phys. Rev. B **56**, 7847 (1997).
- [9] C. Honerkamp and M. Sigrist, J. Low. Temp. Phys. **111**, 895 (1998).
- [10] T. Löfwander, V. S. Shumeiko, and G. Wendin, Supercond. Sci. Technol. **14**, R53 (1997).
- [11] M. J. M. de Jong and C. W. J. Beenakker, Phys. Rev. Lett. **74**, 1657 (1995).
- [12] R. J. Soulen Jr., J. M. Byers, M. S. Osofsky, B. Nadgorny, T. Ambrose, S. F. Cheng, P. R. Broussard, C. T. Tanaka, N. Nowak, J. S. Moodera, A. Barry, and J. M. D. Coey, Science **282**, 282 (1998).
- [13] S. K. M. Upadhyay, A. Palanisami, R. N. Louie, and R. A. Buhrman, Phys. Rev. Lett. **81**, 3247 (1998).
- [14] N. Yoshida, Y. Tanaka, J. Inoue, and S. Kashiwaya, J. Phys. Soc. Jpn. **68**, 1071 (1999); S. Kashiwaya, Y. Tanaka, N. Yoshida, and M. R. Beasley, Phys. Rev. B **60**, 3572 (1999);
- [15] I. Zutic and O. T. Valls, Phys. Rev. B **60** (1999) 6320; **61**, 1555 (2000); J.-X. Zhu, B. Friedman, and C. S. Ting, Phys. Rev. B **59**, 9558 (1999); J.-X. Zhu and C. S. Ting, Phys. Rev. B **61**, 1456 (2000); Z. C. Dong, D. Y. Xing, Z. D. Wang, Z. Zheng, and J. Dong, Phys. Rev. B **61**, 144520 (2001); N. Stefanakis, Phys. Rev. B **64**, 224502 (2001); J. Phys. Condens.Matter **13**, 3643 (2001);
- [16] T. Hirai, Y. Tanaka, N. Yoshida, Y. Asano, J. Inoue, and S. Kashiwaya, Phys. Rev. B **67**, 174501 (2003); I. Zutic, J. Fabian, and S. D. Sarma, Rev. Mod. Phys. **76**, 323 (2004); J. Linder and A. Sudbø, Phys. Rev. B **75**, 134509 (2007); P. H. Barsic and O. T. Valls, Phys. Rev. B **79**, 014502 (2009).
- [17] C. Zener, Phys. Rev. **82**, 43 (1951); P. W. Anderson and H. Hasegawa, Phys. Rev. **100**, 675 (1955); P. G. de Gennes, Phys. Rev. **118**, 141 (1960).
- [18] J. E. Hirsch, Phys. Rev. B **40**, 2354 (1989); **40**, 9061 (1989); **43**, 705 (1991); **59**, 6256 (1999); **62**, 14131 (2000); Physica C **341-348**, 211 (2000).
- [19] D. K. Campbell, J. T. Gammel, and E. Y. Loh, Phys. Rev. B **38**, 12043 (1988); **42**, 475 (1990); S. Kivelson, W.-P. Su, J. R. Schrieffer, and A. J. Heeger, Phys. Rev. Lett. **58**, 1899 (1987).
- [20] Y. Okimoto, T. Katsufuji, T. Ishikawa, A. Urushibara, T. Arima, and Y. Tokura, Phys. Rev. Lett. **75**, 109 (1995); Y. Okimoto, T. Katsufuji, T. Ishikawa, T. Arima, and Y. Tokura, Phys. Rev. B **55**, 4206 (1997); S. Broderick, B. Ruzicka, L. Degiorgi, H. R. Ott, J. L. Sarrao, and Z. Fisk, Phys. Rev. B **65**, 121102 (2002).
- [21] M. Higashiguchi, K. Shimada, K. Nishiura, X. Cui, H. Namatame, and Masaki Taniguchi, Phys. Rev. B **72**, 214438 (2005).
- [22] A. McCollam, S. R. Julian, P. M. C. Rourke, D. Aoki, and J. Flouquet, Phys. Rev. Lett. **94**, 186401 (2005); I. Sheikin, A. Gröger, S. Raymond, D. Jaccard, D. Aoki, H. Harima, and J. Flouquet, Phys. Rev. B **67**, 094420

- (2003).
- [23] G. Annunziata, M. Cuoco, C. Noce, A. Romano, and P. Gentile, *Phys. Rev. B* **80**, 012503 (2009).
- [24] G. Annunziata, M. Cuoco, P. Gentile, A. Romano, and C. Noce, *Phys. Rev. B* **83**, 094507 (2011).
- [25] G. Annunziata, M. Cuoco, P. Gentile, A. Romano, and C. Noce, *Supercond. Sci. Technol.* **24**, 024021 (2011).
- [26] F. Laube, G. Goll, H. v. Löhneysen, F. Fogelström, and F. Lichtenberg, *Phys. Rev. Lett.* **84**, 1595 (2000).
- [27] S. Kashiwaya, H. Kashiwaya, H. Kambara, T. Furuta, H. Yaguchi, Y. Tanaka, and Y. Maeno, *Phys. Rev. Lett.* **107**, 077003 (2011).
- [28] Y. Maeno, H. Hashimoto, K. Yoshida, S. Nishizaki, T. Fujita, J.G. Bednorz, and F. Lichtenberg, *Nature* **372**, 532 (1994).
- [29] K. Ishida, H. Mukuda, Y. Kitaoka, K. Asayama, Z. Q. Mao, Y. Mori, and Y. Maeno, *Nature* **396**, 658 (1998).
- [30] G.M. Luke, Y. Fudamoto, K.M. Kojima, M.I. Larkin, J. Merrin, B. Nachumi, Y.J. Uemura, Y. Maeno, Z.Q. Mao, Y. Mori, H. Nakamura, and M. Sigrist, *Nature (London)* **394**, 558 (1998).
- [31] A.P. Mackenzie and Y. Maeno, *Rev. Mod. Phys.* **75**, 657 (2003).
- [32] K.D. Nelson, Z.Q. Mao, Y. Maeno, and Y. Liu, *Science* **306**, 1151 (2004).
- [33] M. Sigrist, *Prog. Theor. Phys. Suppl.* **160**, 1 (2005)
- [34] Y. Maeno, S. Kittaka, T. Nomura, S. Yonezawa1, and K. Ishida1, *J. Phys. Soc. Jpn.* **81**, 011009 (2012).
- [35] A. Sawa, S. Kashiwaya, H. Obara, H. Yamasaki, M. Koyanagi, N. Yoshida, and Y. Tanaka, *Physica C* **339**, 287 (2000)